J. COMBIN. MATH. COMBIN. COMPUT. 125 (2025) 2761--2774

Journal of Combinatorial Mathematics and Combinatorial Computing
www.combinatorialpress.com/jcmcc

Combinatorial Press

Numerical Linear Algebra for Optimisation Methods in Engineering and Technology Problems

Daming Xu[1,✉]

[1] *Hunan College for Preschool Education, Changde, Hunan, 415000, China*

ABSTRACT

In this paper, the development of blast and shock engineering technology problems using linear algebra's measure analysis is used to make expected judgements through the performance of the data. The problem can be simplified and the frequency stability of the communication transmission system can be optimised by using the data as a benchmark through linear transformations, eigenvectors, matrices and other arithmetic methods. Regularisation and quantisation process the image to improve the science and accuracy of large-scale image restoration algorithm operation. It has been shown that the optimised prediction formula is very consistent with the experimental results in blasting experiments with a building as the object of study. The frequency drift of the optimised laser is reduced from 850 MHz to 160 MHz. the acquired noise intensity is optimal at different communication transmission moments, and the highest noise intensity acquired at frequency is 0.097 dB. The stability is optimal at different times of communication signal switching. The regularisation optimised ship navigation images have the largest values of structural similarity and information entropy metrics.

Keywords: magnitude analysis, linear algebra, image restoration, regularisation process

1. Introduction

In recent years, with the continuous development of engineering and construction, the theoretical knowledge used in various projects has undergone tremendous innovation. Architectural engineering technology belongs to the project construction is very important in some of the technology, and has a strong application, these technologies to the process of national economic construction supply an important service [1-3]. The close integration of engineering technology and practical production is one of the more active branches in the surveying and mapping disciplines, and a part of the university has offered linear algebra courses in engineering majors [4-6]. Linear algebra theoretical system is the basis of many disciplines, many technologies are built on the framework of linear algebra theory, people are committed to the original concepts on the basis of constantly expanding the numerical operations in the new concepts and their computational methods, in order to obtain better

✉ Corresponding author.
E-mail address: cd_1498@163.com (D. Xu).
Received 10 March 2024; Revised 15 May 2024; Accepted 05 December 2024; Published Online 15 April 2025.
DOI: 10.61091/jcmcc127a-156

computational results in practice [7-9]. “Numerical linear algebra” is a special course for information and computational science majors in colleges and universities, as the core of scientific and engineering computation, it has both the abstraction and rigor of various specialized courses in mathematics, as well as the technology and application of solving practical problems, and its important role in cultivating applied innovative talents is self-evident [10-12]. Through the study of some practical projects in recent years, it can be seen that a large number of practical engineering technology problems have been applied numerical linear algebra for processing [13-14]. On the one hand, engineering technology belongs to the technical content, which is based on physics and mathematics, and uses the fundamental theories, techniques and relevant methods of surveying and mapping science to supply the support of measurement technology for engineering construction [15-17]. On the other hand, in engineering technology, mathematics is fundamental and a condition for good study of technical specialties, so the study of optimization methods of numerical linear algebra is of great significance for solving engineering technology problems in specific projects [18-20].

In this paper, through theoretical analysis, we study the mathematical properties of vectors, matrices and other mathematical properties, as well as the algorithms between them, which are widely used in engineering and technical problems. The original complex problem of measure analysis is transformed into a matrix arithmetic problem that can be solved quickly and easily with the help of computer algebra system. A linear space description of magnitude analysis is established, and an example of the application of the above method in the field of explosion and impact engineering research is given. The regularization method based on numerical linear algebra is applied to optimize the restored ship navigation images, so as to obtain high-quality ship navigation images. Finally, the method of linear algebra model optimization of LiDAR communication frequency is designed to complete the control and optimization of communication frequency.

2. Examples of applications in blast and shock engineering optimisation studies

The use of solving systems of equations to deal with large amounts of data in real engineering applications and to propose better data decisions. In the teaching of linear algebra, matrix and system of equations is the core of teaching, in the actual construction engineering, a large amount of data to meet the relevant system of equations need to be linear algebra knowledge to solve. In dealing with the actual project, to fully integrate the eigenvalue, eigenvector solution principle, the use of eigenvalue eigenvector can establish continuous or discrete differential equations, better predict the project in the process of construction in which aspects need to be strengthened to deal with the structural mechanics and the layout of the project should be in accordance with the resulting linear equations to design, so as to ensure the quality of the project and safety.

2.1. Theoretical basis for the ‘overpressure-impulse’ damage criterion for shock waves

Shock wave on the building structure of the damage effect or damage level of the determination of the more widely recognized method is to use the “overpressure - impulse” damage criterion (known as the “P-I” criterion), the current engineering is widely used in the following formulas to describe:

$$(P-P_{cr})(I-I_{cr})=A\left(\frac{P_{cr}}{2}+\frac{I_{cr}}{2}\right)^{B} \tag{1}$$

Where A, B are dimensionless constants, P, I are the overpressure and impulse of the shock wave acting on the building structure, and P_{cr}, I_{cr} are the overpressure and impulse damage thresholds of the building structure.

Therefore, strictly speaking, the use of formula (1) to describe the damage of the shock wave on the building structure in the theory is not rigorous.

Building structure by the action of the shock wave generated by the displacement of y, assuming that the shock wave overpressure peak for P, the impulse for I, positive pressure time for t_d, the characteristic mass of the building structure for M, the stiffness of K, the building structure is completely destroyed by the displacement generated by y_c, the building structure of the level of damage with "the building structure to a certain degree of damage generated by the displacement (damage displacement) y is characterized by the ratio of the displacement produced when it is completely destroyed", and with a damage class of D, we have $D=\frac{y}{y_c}$. It is obvious that $D \in [0,1]$: when $D=1$, the damage level is the highest, and the building structure is completely destroyed. At $D=0$, the damage level is the lowest and the structure is not damaged at all. It is required to give a qualitative functional relationship characterizing D.

For building structures, a widely used physical quantity to characterise the damage effect of shock waves is the damage displacement y. Analysing this, it can be seen that the magnitude of y can be fully determined by the following physical quantities.

Properties of the building structure: mass M, stiffness K, displacement in case of total destruction y_c, characteristic dimensions of the building L.

Shock wave characteristics: overpressure P, positive pressure action time t_d, impulse I.

In order to simplify the process of magnitude analysis, the two physical quantities of shock wave positive pressure action time t_d and building characteristic size L can be omitted by further physical analysis for the following reasons:

1) In engineering, the triangle approximation is usually used to find the shock wave impulse, i.e., there is:

$$I = \frac{1}{2} P t_d \tag{2}$$

Thus, t_d can be completely determined by P and I, and since we have explicitly had to consider the physical quantities P and I in our quantitative analysis, t_d can be disregarded.

2) Obviously, L and y_c are of the same magnitude, and for the specified building structure, it is easy to understand that L and y_c are proportional, i.e., L can be represented by y_c. Therefore, only physical quantity y_c can be taken into account when analysing the magnitude, instead of physical quantity L.

It is easy to analyse that the basic quantities involved in the above related physical quantities are length, mass and time, and their magnitudes are L, M and T, so there are $n=5$ independent variables and $k=3$ basic quantities, and y is the dependent variable and M, K and y_c are the reference quantities to obtain the magnitude matrices A and B as follows:

$$A = \begin{bmatrix} 0 & 1 & 0 \\ 0 & 1 & -2 \\ 1 & 0 & 0 \end{bmatrix}, B = \begin{bmatrix} 1 & 0 & 0 \\ 0 & 1 & 0 \\ 0 & 1 & -2 \\ 1 & 0 & 0 \\ -1 & 1 & -2 \\ -1 & 1 & -1 \end{bmatrix} \tag{3}$$

With the help of a computer algebra system the measure matrix M is obtained as follows:

$$M = BA^{-1} = \begin{bmatrix} 0 & 0 & 1 \\ 1 & 0 & 0 \\ 0 & 1 & 0 \\ 0 & 0 & 1 \\ 0 & 1 & -1 \\ 1/2 & 1/2 & -1 \end{bmatrix} \tag{4}$$

The essential dimensionless independent variables are obtained using matrix (4) as follows:

$$\begin{cases} \pi_1 = \dfrac{P}{M^0 K^1 y_c^{-1}} = \dfrac{P}{K/y_c} \\ \pi_2 = \dfrac{I}{M^{1/2} K^{1/2} y_c^{-1}} = \dfrac{I}{\sqrt{MK}/y_c} \end{cases} \tag{5}$$

Similarly, the essential dimensionless dependent variable is:

$$\pi_0 = \frac{y}{M^0 K^0 y_{\mathrm{c}}^1} = \frac{y}{y_{\mathrm{c}}} \tag{6}$$

The dimensionless functional equation is obtained as follows:

$$\pi_0 = \psi(\pi_1, \pi_2) \Rightarrow \frac{y}{y_c} = \psi\left(\frac{P}{K/y_c}, \frac{I}{\sqrt{MK}/y_c}\right) \tag{7}$$

The above equation shows that π_0 is a function about π_1, π_2. Thus, numerical simulation based on the experimental and numerical simulation results gives π_0 curves about π_1, π_2.

2.2. Feasibility and efficiency

The results of the comparison between the analytical prediction formula and the experimental data are given as an example of a building blasting experiment. The comparison results are shown in Figure 1. The bar graph represents the experimental results, and the curve represents the prediction formula, which shows that the optimised prediction formula after linear algebra conforms well to the experimental results, with an accuracy value of about 90%, and at the same time proves the feasibility and efficiency of the algorithm.

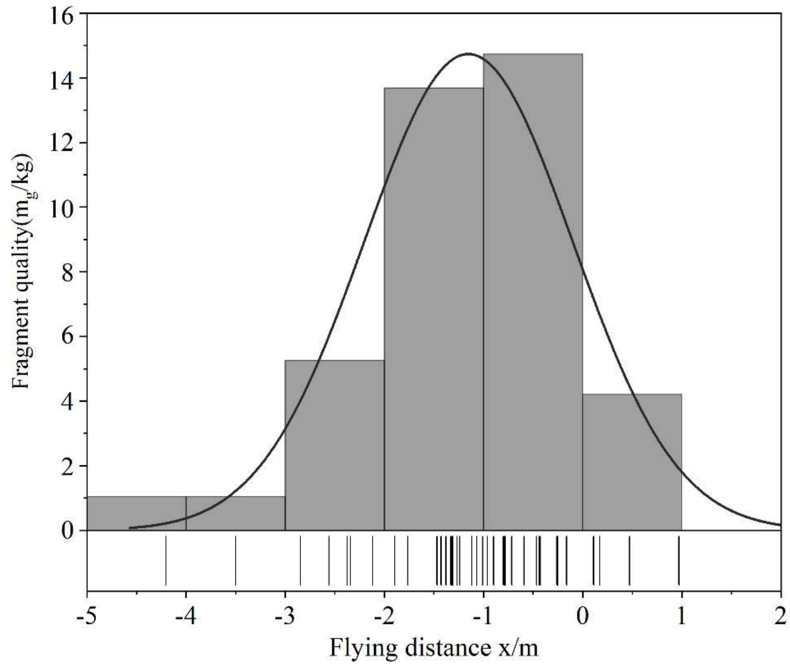

Fig. 1. The quality distribution pattern compares results

3. Optimisation of the linear algebraic model of the transmission frequency of lidar communications

3.1. *Linear Algebraic Optimisation Models*

The basic principle of LIDAR ranging. The frequency of the transmitted signal varies linearly up and down periodically with time, the rise time is the same as the fall time, and the average value of the frequency is f_c. The transmission delay from the collimator to the target to be measured and then scattered back to the receiving end is denoted as τ, and the variation range of the signal frequency is denoted as the bandwidth B. Due to the linear variation of the signal frequency with time and the Doppler effect generated by the relative displacement of the measured target, a frequency difference df is generated between the frequency of the received echo signal and the frequency of the local oscillator signal, which consists of the amount of frequency variation f_R introduced due to the distance delay τ and the Doppler shift f_D, which differs f_D between each of the frequency difference Δf_1 generated at the rising edge of the frequency and the frequency difference Δf_2 generated at the falling edge of the frequency and f_R. Then the differential frequency quantity f_R and the Doppler shift f_D introduced by the distance can be calculated from Δf_1 and Δf_2 by means of coherent demodulation:

$$\begin{cases} f_R = \dfrac{\Delta f_1 + \Delta f_2}{2} \\ f_D = \dfrac{\left|\Delta f_1 - \Delta f_2\right|}{2} \\ \gamma = \dfrac{B}{T/2} = \dfrac{2B}{T} \\ \tau = \dfrac{f_R}{\gamma} = \dfrac{\left(\Delta f_1 + \Delta f_2\right)T}{4B} \end{cases} \tag{8}$$

$$\Rightarrow \begin{cases} R = \dfrac{c \cdot \tau}{2} = \dfrac{c \cdot f_R}{2\gamma} = \dfrac{c\left(\Delta f_1 + \Delta f_2\right)T}{8B} \\ v = \dfrac{f_D \cdot c}{f_c} \end{cases}$$

Where: γ represents the rate of change of the frequency of the transmitted signal, R represents the distance between the LIDAR and the target, c represents the speed of light, v represents the projection of the target velocity on the line between the LIDAR and the target, and f_c represents the centre frequency of the optical carrier of the transmitted signal. As a result, the distance R and the relative speed v of the measured target can be demodulated.

By analysing the system of linear algebra equations, the resulting massive data are matrix processed, followed by matrix partitioning and LU decomposition to transform the large matrix data into small pieces of matrices. At the same time, the obtained target matrix is transformed into the product of matrix L and matrix U. L and U are upper and lower triangular matrices, respectively. In this way, the target matrix Q=LU is processed and mined for in-depth data processing in order to complete the frequency stabilisation optimisation of the communication transmission system.

3.2. Optimisation performance testing

In order to test the optimisation performance of this method, the results of the change in the output communication frequency of the frequency stabilisation device before and after optimisation are measured and counted, and the results are shown in Figure 2. According to the test results, it can be seen that: the maximum communication frequency drift generated by the laser in 60 min before optimisation is about 850 MHz. the frequency output drift after optimisation, it can be seen that the maximum drift of the communication frequency generated by the laser in 60 min is about 160 MHz. therefore, comparing with the test results, it can be seen that the frequency drift of the laser after optimisation is reduced from 850 MHz to 160MHz, indicating that the optimisation of this method can effectively reduce the frequency drift generated by the LiDAR in the process of communication transmission, reduce the frequency fluctuation, and ensure the stability of the communication transmission frequency.

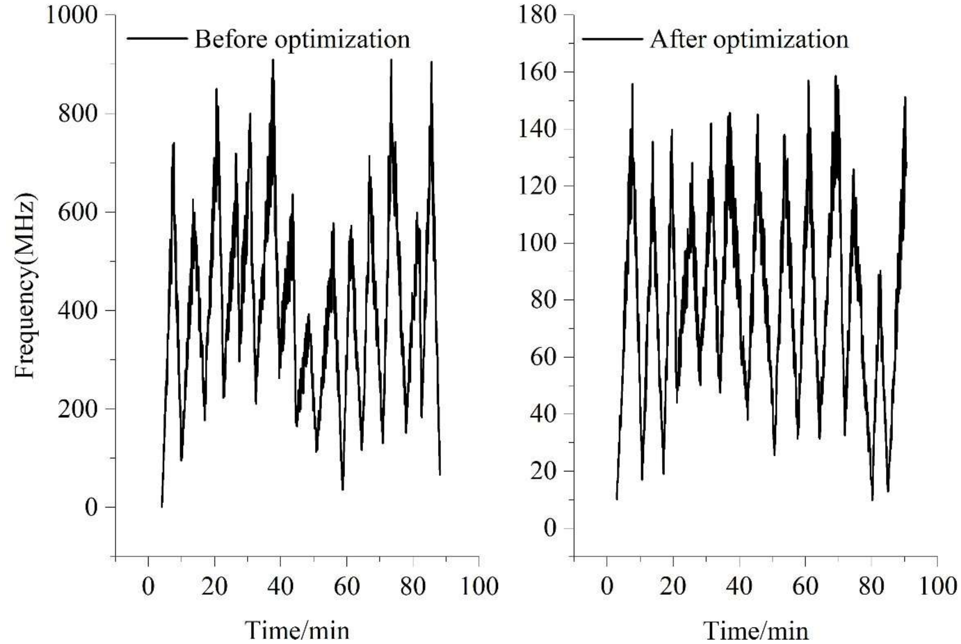

Fig. 2. Change of output communication frequency of stable frequency device

3.3. Noise Suppression Performance Test

Lidar will be affected by different noises during the communication transmission process, therefore, the noise suppression performance of Lidar communication transmission after optimisation of this method is analysed, and the carrier frequency stabilisation control method and the multi-band signal source remote switching control method of the distributed communication network in the relevant optical communication are compared with the present method, and the three methods are statistically used to obtain the noise of the communication transmission frequency within different transmission moments. The intensity and the allowed communication time lag, and the results are shown in Table 1. Among them, the higher the noise intensity acquired by the communication transmission frequency proves that the noise suppression performance is better.

Analysing the test results in the table, it can be seen that: the noise intensity acquired by the communication transmission frequency of this method is the best in different communication transmission moments, and the highest noise intensity acquired by the frequency is 0.097dB, and the allowable communication time lag is the smallest, which is within 0.145s. The communication transmission frequency acquired noise intensity of both comparison methods is significantly lower than that of the present method, with the highest frequency acquired noise intensity of 0.063 dB and 0.065 dB, respectively, and the allowable communication time lag is more than 0.210 s. Therefore, it is shown that the present method is better optimised to improve the noise suppression performance of LiDAR communication transmission.

Table 1. The noise suppression of the three methods compares the results

Method category	Hour/s	Noise intensity of frequency acquisition/dB	Allowable communication delay/s
This method	10	0.086	0.130
	15	0.089	0.135
	20	0.094	0.142
	25	0.097	0.145
Carrier frequency stability control method in relevant optical communication	10	0.056	0.211
	15	0.057	0.214
	20	0.060	0.213
	25	0.063	0.210
Distributed communication network	10	0.062	0.207
	15	0.063	0.206
	20	0.060	0.213
	25	0.065	0.210

3.4. Applied testing

Using the above linear algebraic equation optimisation method frequency stabilisation device for communication transmission frequency regulation, test the application of this method, communication transmission frequency regulation results, the device implements the frequency spectrum of communication transmission as shown in Figure 3. When the frequency is 69.99~70.01MHz, the RF energy reaches the highest value of more than 10/dBm. This ensures the stability of the communication output frequency.

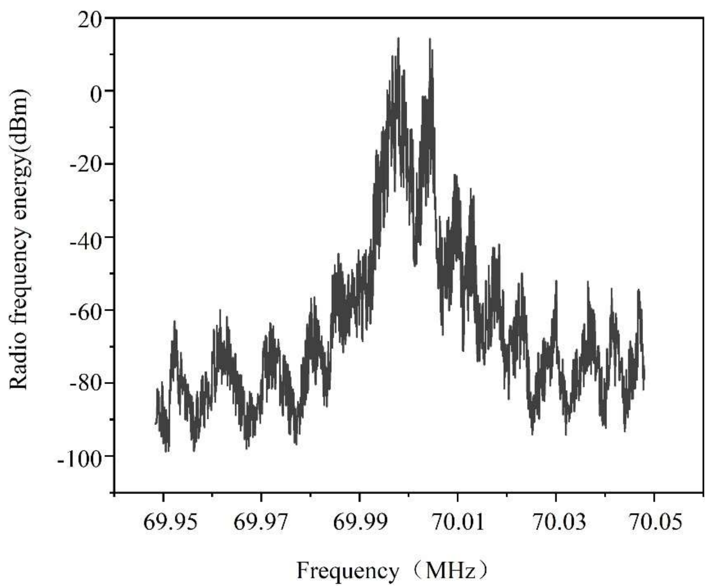

Fig. 3. The communication spectrum of the stationary frequency device

Test the frequency control performance of the communication transmission signal at the time of switching after the application of this method, and test the fluctuation of the signal transmission power of the three methods at the time of switching of the communication transmission as well as the change of the signal-to-noise ratio, and the results are shown in Table 2. Test results: the signal transmission power of the three methods is consistent and unchanged at different times before the communication signal switching. When switching hair, the signal transmission power of the present method is extremely small compared with that before switching, and the maximum change of signal transmission power is 7.33 dBm, which is relatively stable. This result shows that after the application of this method, the frequency stability of LiDAR communication signal switching can be effectively ensured, and the application performance is good.

Table 2. Test results of three methods

Test content	Initial signal	This method	Carrier frequency stability control method in relevant optical communication	Distributed communication network
Signal transmission power /dBm	Before switching 2s	-93.47	-92.48	-92.48
	Before switching 4s	-91.28	-90.85	-90.77
	Before switching 6s	-90.25	-90.26	-90.26
	After switching 2s	-87.26	-64.48	-66.38
	After switching 4s	-86.39	-25.25	-27.28
	After switching 6s	-86.14	-83.67	-81.67
Signal-to-noise ratio/dB	Before switching 2s	7.24	8.20	7.54
	Before switching 4s	6.32	8.89	8.26
	Before switching 6s	5.04	9.37	9.17
	After switching 2s	11.96	16.59	15.49
	After switching 4s	10.86	1.46	1.28
	After switching 6s	10.79	14.08	13.45

4. Ship navigation image optimisation

Ship navigation image acquisition is easily affected by factors such as hazy weather and ship navigation status, which leads to problems such as blurring or even deformation of the acquired image, resulting in a significant reduction in the quality of ship navigation images and making it difficult to realise the subsequent application of ship navigation images.

Define the project as a two-dimensional function $w(x,y)$, x,y represent the horizontal and vertical coordinates of the picture pixels, respectively, and locate the light intensity and grey scale of the image at this position by x,y. The two-dimensional function $w(x,y)$ is used to transform the image into a digital information image so that in-depth image processing can be performed. In the transformation process, the space x, y, and w are finite. The mathematical matrix associated with the image is obtained by regularisation process and quantisation process. The processing of the image is to remove the redundant data from the image and retain the data that is useful for the image for better and efficient data storage and transmission.

4.1. Linear Algebra Regularisation Methods

Regularisation methods that introduce certain a priori information about the restored image (such as smoothness and sparsity, etc.) are effective methods for solving ill-defined image restoration problems. Commonly used regularisation methods are divided into direct regularisation methods and iterative regularisation methods.

Direct regularisation methods include Truncated Singular Value Decomposition (TSVD for short), Selected Singular Value Decomposition and Tikhonov's method, etc. The TSVD method is obtained by discarding the noise-dominated SVD component:

$$f_{tsvd} = \sum_{i=1}^{k} \frac{u_i^T g}{\sigma_i} v_i \tag{9}$$

The classical Tikhonov regularisation model is:

$$\arg\min_f \left\{ \|Kf - g\|_2^2 + \alpha \|Df\|_2^2 \right\} \tag{10}$$

where D is the regularisation matrix, usually the unit matrix or the discrete approximation matrix of the difference operator, and α is called the regularisation parameter. If D is the unit matrix, the solution of Tikhonov's method can be expressed as:

$$f_{tik} = \sum_{i=1}^{n} \frac{\sigma_i^2}{\sigma_i^2 + \alpha^2} \frac{u_i^T g}{\sigma_i} v_i \tag{11}$$

Recent advances in direct regularisation methods can be found in further References.

Direct regularisation methods are very effective in solving small and medium scale linear discrete ill-posed problems, however, they are not suitable for large scale linear discrete ill-posed problems due to the need to compute the singular value decomposition of the matrix. The iterative regularisation method is suitable for solving large-scale linear discrete ill-posed problems because the product of large-scale fuzzy matrices and vectors with special structure can be implemented quickly. In addition, the difference principle in the framework of the iterative regularisation method enables the number of iterations of the iterative regularisation method to be determined in real time. Classical iterative regularisation methods include Landweber methods, algebraic reconstruction methods and Krylov subspace methods, which are the most popular iterative regularisation methods, including LSQR methods, GMRES methods and CGLS methods. Its core is to solve the following problem:

$$\arg\min_f \left\{ \|Kf - g\|_2 ,\ s.t. f \in \mathrm{K}_k \right. \tag{12}$$

where K_k is a Krylov subspace.

The Krylov subspace is usually:

$$\mathrm{K}_k := span\left\{ g, Kg, K^2 g, \cdots, K^{k-1} g \right\} \tag{13}$$

Or:

$$\mathrm{K}_k := span\left\{ K^T g, \left(K^T K\right) K^T g, \left(K^T K\right)^2 K^T g, \cdots, \left(K^T K\right)^{k-1} K^T g \right\} \tag{14}$$

The basis vectors of the above Krylov subspace can be obtained by the Arnoldi process and the Lanczos bi-diagonalisation process respectively.

The Lanczos bi-diagonalisation process (i.e., the Golub-Kahan bi-diagonalisation process) is described as follows:

Set the unit initial vectors $\beta_1 = \|g\|_2$, $u_1 = g/\beta_1$ and $v_0 = 0$.

$$for\ k = 1, 2, \cdots \tag{15}$$

$$v_k = K^T u_k - \beta_k v_{k-1} \tag{16}$$

$$\alpha_k = \|v_k\|_2 \tag{17}$$

$$v_k = v_k / \alpha_k \tag{18}$$

$$u_{k+1} = K v_k - \alpha_k w_k \tag{19}$$

$$\beta_k = \|u_{k+1}\|_2 \tag{20}$$

$$u_{k+1} = u_{k+1} / \beta_k \tag{21}$$

After the k-step Lanczos bi-diagonalisation process, the lower bi-diagonal matrix $B_k \in \mathbb{R}^{(k+1)\times k}$ is obtained and the column orthogonal matrices $U_{k+1} \in \mathbb{R}^{m\times(k+1)}$ and $V_k \in \mathbb{R}^{n\times k}$ satisfy the following relations:

$$KV_k = U_{k+1} B_k, K^T U_{k+1} = V_k B_k^T + \alpha_{k+1} v_{k+1} e_{k+1}^T \tag{22}$$

Iterative regularisation methods are suitable for solving large-scale linear discrete ill-posed problems, however most iterative regularisation methods suffer from semi-convergence. That is, affected by noise, the relative error of the solution of an iterative regularisation method quickly decreases to a minimum as the number of iterations increases but then starts to increase rapidly. Suffering from the phenomenon of semi-convergence, iterative regularisation methods are likely to give very poor results if there is no excellent termination criterion.

Image Sparse Representation Theoretical studies have shown that there always exists a sparse representation of images in the real world under suitable bases (e.g., orthogonal systems, tight frames, etc.) or dictionaries. That is, a real-world image can be described by a linear combination of a very small number of atoms (atom) in the basis or dictionary, where most of the coefficients are zero, and there are only a few non-zero coefficients that reflect the nature of the image. The sparse nature of images in the real world provides new ideas for further designing efficient algorithms applicable to large-scale image restoration problems. The development and maturity of sparse optimisation algorithms (convex and non-convex optimisation algorithms) for solving sparse regularised image restoration models have also driven research based on sparse regularisation models. Sparse regularised image restoration models with elegant mathematical frameworks are introduced in the following, including the full variance (abbreviated as TV) based image restoration model and the tight frame based image restoration model.

The full variance based image restoration model is as follows:

$$\min_f \|Kf - g\|_2^2 + \alpha \|\nabla f\|_2 \tag{23}$$

where the regularisation parameter $\alpha > 0$ balances the fidelity term and the regularisation term. Recent advances in regularisation methods that exploit the sparse properties of real-world image gradients can be further referenced.

Tight frame image restoration based models:

1) Synthetic model:

$$\min_d \|K\mathrm{R}\, d - g\|_2^2 + \alpha \|d\|_1 \tag{24}$$

2) Analytical models:

$$\min_f \|Kf - g\|_2^2 + \alpha \|\mathrm{R}^T f\|_1 \tag{25}$$

3) Equilibrium modelling:

$$\min_d \left\| K\mathrm{R}\, d - g \right\|_2^2 + \alpha_1 \left\| d \right\|_1 + \alpha_2 \left\| \left(I - \mathrm{R}^T \mathrm{R} \right) d \right\|_2^2 \tag{26}$$

where $f = \mathrm{R}\, d$, $\mathrm{R} \in \mathbb{R}^{n\times m}$ are synthetic operators.

The sparse nature of real-world images provides new ideas for further designing high-performance algorithms applicable to large-scale image restoration problems. The mainstream method for solving sparse regularised image restoration models is the split-iteration method, whose core idea is divide-and-conquer. The core idea is to split the complex numerical algebra problem or optimisation problem (including non-trivial terms, non-convex terms, etc.) into several easy-to-solve sub-problems (e.g., linear algebra system with special structure, non-linear sub-problems with explicit solutions, etc.). Split iterative methods for solving full variational image restoration based models can be categorised as primal algorithms, dyadic algorithms and primal-dyadic algorithms. Excellent primal algorithms include the FTVd algorithm, the split Bregman algorithm, the augmented Lagrangian algorithm, the neighbourhood split algorithm, etc. Pairwise algorithms transform certain primal problems that are difficult to solve into easier pairwise problems to solve. Considering that primal and dyadic problems have their own difficulties, primal-dyadic algorithms utilise both primal and dyadic variable information to improve the performance of the algorithm.

4.2. Optimising visual effects

Structural similarity (SSIM) and information entropy are important indexes for evaluating the visual effect of images, the former reflects the degree of consistency between the optimised image and the clear image, and the latter measures the amount of information contained in the optimised image, and the larger the value of the two indexes, the more prominent is the effect of optimising the visual communication of ship navigation images. Seven blurred ship navigation images are randomly selected from the data set and visually optimised using this paper's method, and the visual optimisation performance of this paper's method is verified by comparing and analysing the differences in structural similarity and information entropy index values between the deblurred and visually optimised images and the clear ship navigation images, and the experimental results are shown in Table 3. It can be seen that the structural similarity index value between the regularized optimized ship navigation image and the clear ship navigation image is between [0.916,0.974], and the minimum value of the information entropy index is 9.25, and the maximum value is 9.50. The maximum value of the structural similarity index between the deblurred ship navigation image and the clear image is 0.949, and the minimum value is 0.908, and the maximum value of the information entropy index is 9.47, and the minimum value is 9.47, respectively. The maximum and minimum values of the information entropy index are 9.47 and 9.15 respectively, and it is found that the regularisation optimisation can effectively improve the quality of ship navigation images, and the values of the two indexes have been improved to a certain extent. The experimental results show that the method in this paper has the performance of visual communication optimisation for ship navigation images, and the visual effect of images is significantly improved.

Table 3. Visual optimization performance analysis of the method in this article

Navigation image number	Visual optimization		Blur	
	Structural similarity	Information entropy	Structural similarity	Information entropy
A0052	0.937	9.25	0.914	9.17
A0114	0.947	9.42	0.912	9.38
A0275	0.916	9.30	0.908	9.15
A0611	0.948	9.40	0.928	9.34
A0725	0.960	9.50	0.947	9.47
A0967	0.974	9.42	0.949	9.22
A1238	0.928	9.41	0.915	9.34

5. Conclusion

Linear algebra can be used to optimise and solve many practical problems, and this paper takes three practical cases, namely, the damage effect or damage level of shock wave on building-type structures, communication transmission frequency and ship sailing image, as the research objects, and accepts the application and optimisation method of linear algebra in the cases. The results show that in a building blasting experiment, the optimised prediction formula of linear algebra is consistent with the actual experimental results, and can accurately predict the destructive effect or destructive grade in the blasting experiment. Laser Lidar communication transmission frequency is reduced by 690 MHz after optimisation. Transmission power and before and after switching, the optimised signal transmission power is more stable with little change. The information entropy index of the ship navigation image after regularisation optimisation is the largest, and the method proposed in this paper has the best visual optimisation effect.

References

[1] Zavadskas, E. K., Antucheviciene, J., Vilutiene, T., & Adeli, H. (2017). Sustainable decision-making in civil engineering, construction and building technology. Sustainability, 10(1), 14.

[2] Zavadskas, E. K., Šaparauskas, J., & Antucheviciene, J. (2018). Sustainability in construction engineering. Sustainability, 10(7), 2236.

[3] Radziszewska-Zielina, E., Kania, E., & Śladowski, G. (2018). Problems of the selection of construction technology for structures in the centres of urban agglomerations. Archives of Civil Engineering, 64(1).

[4] Peng, W. (2019). Research on the Construction of Curriculum System of Surveying Technology Specialty Semester in Higher Vocational Colleges. Advances in Vocational and Technical Education, 1(1), 1-4.

[5] Blyth, T. S. (2018). Module theory: an approach to linear algebra. University of St Andrews.

[6] Silva, M., Hieronymi, P., West, M., Nytko, N., Deshpande, A., Chuang, J. C., & Hilgenfeldt, S. (2022, August). Innovating and modernizing a Linear Algebra class through teaching computational skills. In 2022 ASEE Annual Conference & Exposition.

[7] Farin, G., & Hansford, D. (2021). Practical linear algebra: a geometry toolbox. Chapman and Hall/CRC.

[8] Martinsson, P. G., & Tropp, J. A. (2020). Randomized numerical linear algebra: Foundations and algorithms. Acta Numerica, 29, 403-572.

[9] Trefethen, L. N., & Bau, D. (2022). Numerical linear algebra. Society for Industrial and Applied Mathematics.

[10] Strang, G. (2022). Introduction to linear algebra. Wellesley-Cambridge Press.

[11] Axler, S. (2024). Linear algebra done right (p. 390). Springer Nature.

[12] Harel, G. (2017). The learning and teaching of linear algebra: Observations and generalizations. The Journal of Mathematical Behavior, 46, 69-95.

[13] Hager, W. W. (2021). Applied numerical linear algebra. Society for Industrial and Applied Mathematics.

[14] Ibañez, R., Borzacchiello, D., Aguado, J. V., Abisset-Chavanne, E., Cueto, E., Ladeveze, P., & Chinesta, F. (2017). Data-driven non-linear elasticity: constitutive manifold construction and problem discretization. Computational Mechanics, 60, 813-826.

[15] Uren, J., & Price, B. (2018). Surveying for engineers. Bloomsbury Publishing.

[16] Rizos, C. (2017). Surveying. Springer Handbook of Global Navigation Satellite Systems, 1011-1037.

[17] Guangyun, L. I., & Baixing, F. A. N. (2017). The development of precise engineering surveying technology. Acta Geodaetica et Cartographica Sinica, 46(10), 1742.

[18] Gill, P. E., Murray, W., & Wright, M. H. (2021). Numerical linear algebra and optimization. Society for Industrial and Applied Mathematics.

[19] Abdelfattah, A., Anzt, H., Boman, E. G., Carson, E., Cojean, T., Dongarra, J., ... & Yang, U. M. (2021). A survey of numerical linear algebra methods utilizing mixed-precision arithmetic. The International Journal of High Performance Computing Applications, 35(4), 344-369.

[20] Bianchini, B. L., de Lima, G. L., & Gomes, E. (2019). Linear algebra in engineering: an analysis of Latin American studies. ZDM, 51(7), 1097-1110.